Journal of Statistical Physics, Vol. 27, No. 1, 1982

Two- and Three-Spin Triangular Ising Model: Variational Approximations

A. Malakis[1,2]

Received April 20, 1981

The implications of the known hard-hexagon lattice gas results for the triangular Ising model with both pair and triplet interactions are pointed out. Employing an appropriate generalization of the variational method of Baxter we determine, using the lowest-order approximation, the phase boundaries for this model when the pair interactions are ferromagnetic. Higher approximations are presented for the case of pure triplet interactions and the resulting phase diagrams are in excellent agreement with all exactly known results.

KEY WORDS: Triangular Ising model; hard-hexagon model; variational approximations; phase diagrams.

1. INTRODUCTION

The study of two-dimensional Ising spin models has been one of the most successful attempts to understand the nature of phase transitions. Given a model Hamiltonian, for some lattice spin system, one would like to be able to answer some interesting questions. Such questions concern the existence and extent of phase transitions between different phases of the system, the number and the order of phase transitions for a given "external field," the behavior of the magnetization along the phase boundaries. In this paper we shall try to answer some of these questions for the triangular lattice model specified by the Hamiltonian

$$\mathcal{H} \equiv \sum_{(i,j,k)} h(\sigma_i, \sigma_j, \sigma_k)$$

$$\equiv \sum_{(i,j,k)} \left[-\frac{H}{6}(\sigma_i + \sigma_j + \sigma_k) - \frac{J_2}{2}(\sigma_i\sigma_j + \sigma_i\sigma_k + \sigma_j\sigma_k) - J_3\sigma_i\sigma_j\sigma_k \right] \quad (1)$$

[1] Institutt for Teoretisk fysikk, 7034 Trondheim-NTH, Norway.

[2] Present address: University of Athens, Division of Mechanics, Panepistimiopolis, Athens 621, Greece.

0022-4715/82/0100-0001$03.00/0

Here $\sigma_i, \sigma_j, \sigma_k$ have values $+1$ and -1; each triplet (i, j, k) surrounds an elementary triangle; $h(a, b, c)$ is the contribution to the Hamiltonian of an elementary triangle; and the summation is over all $2N$ triangles (N being the number of sites of the triangular lattice). The partition function is

$$Z_N = \sum_{\{\sigma\}} \exp\left(-\frac{1}{K_B T}\mathcal{H}\right) = \sum_{\{\sigma\}} \prod_{(i,j,k)} w(\sigma_i, \sigma_j, \sigma_k) \tag{2}$$

where $w(a, b, c) = \exp[-(1/K_B T)h(a, b, c)]$ is the Boltzmann weight of any interacting triplet (a, b, c) and the summation is over all 2^N spin configurations of the Ising system. We will have to deal with the partition function per site, in the thermodynamic limit,

$$k = \lim_{N\to\infty} Z_N^{1/N} \tag{3}$$

The model described by the Hamiltonian (1) is particularly interesting as an example of spin systems without the usual up–down spin reversal symmetry.[1–5] [(1) is invariant under the transformation $H \to -H$, $J_3 \to -J_3$ and $\sigma_i \to -\sigma_i$, therefore, without loss of generality, we will consider $J_3 \leqslant 0$.] This model incorporates two exactly solvable cases; the Onsager solution ($J_3 = H = 0$) and the Baxter–Wu solution ($J_2 = H = 0$). Furthermore, the hard-hexagons problem, recently solved by Baxter,[6] is obtained from (1) as a "limit" case. The usual way to obtain this equivalence is to consider $J_3 = 0$, $J_2 < 0$ and let $-J_2/K_B T$ and $H/K_B T$ both tend to infinity, keeping

$$z = \exp\left[(-12J_2 - 2H)/K_B T\right] \tag{4}$$

fixed, then the antiferromagnetic triangular Ising model becomes the hard-hexagons lattice gas with activity z, and the critical activity z_c determines the slope of the phase boundary at critical field ($H_c = \pm 6J_2$). However, similar arguments apply when $J_3 \neq 0$ and there are several cases where the slope of the corresponding phase diagrams are determined by z_c. These cases together with the ground state properties of model (1) constitute the subject of the next section.

In cases where no exact information is available one has to resort to approximations. Approximate treatments have a long and rather successful record in the theory of phase transitions. A recent development in this direction is the variational method of Baxter.[7] The method has been applied to some models[8–12] and yielded very accurate results. The main idea of the method is to derive a set of matrix equations from which k may be determined. If the matrices involved have infinite size the equations are exact (corner transfer matrix equations); by restricting the matrices to be finite, a sequence of approximations converging to the exact results is obtained. For "ferromagnetic" triangular models the matrix equations were given by Baxter and Tsang.[11] However, in order to study the critical

properties of the general Hamiltonian (1) one has to distinguish between the three sublattices of the triangular lattice. The necessity for distinction between the sublattices can be seen from the ground state properties; for certain values of H, J_2, and J_3 the system admits a ground state in which spins on one sublattice are down (-1), whereas spins on the other two are up $(+1)$. Such models for which the lattice symmetry may be broken at low temperatures and one of the three sublattices "preferentially occupied" may be referred as "antiferromagnetic" (the model may be "antiferromagnetic" even with ferromagnetic pair interactions $J_2 > 0$). The appropriate generalization of the variational method for "antiferromagnetic" triangular models has been obtained in a previous paper[13] (hereafter referred to as I) and will be stated in Section 3. The variational method is utilized in Section 4, where we restrict ourselves to $J_2 > 0$ and obtain phase diagrams for several values of $r = |J_3|/|J_2|$. Higher approximations are presented for the case of pure triplet interactions ($J_2 = 0$).

2. EXACT PROPERTIES

In order to examine the ground state configurations it is convenient to define

$$r = |J_3|/|J_2| \tag{5}$$

$$H^* = H/(|J_3| + |J_2|) \tag{6a}$$

and

$$h^*(a,b,c) = h(a,b,c)/(|J_3| + |J_2|) \tag{6b}$$

From the definition of the Hamiltonian (1) it is seen that there are four configurations on an elementary triangle with different energies, i.e.,

$$h_1^* = h^*(+,+,+) = -\tfrac{1}{2}H^* + (r - \tfrac{3}{2}a)/(r+1) \tag{7a}$$

$$h_2^* = h^*(+,+,-) = h^*(+,-,+) = h^*(-,+,+)$$
$$= -\tfrac{1}{6}H^* + (-r + \tfrac{1}{2}a)/(r+1) \tag{7b}$$

$$h_3^* = h^*(+,-,-) = h^*(-,+,-) = h^*(-,-,+)$$
$$= \tfrac{1}{6}H^* + (r + \tfrac{1}{2}a)/(r+1) \tag{7c}$$

$$h_4^* = h^*(-,-,-) = \tfrac{1}{2}H^* + (-r - \tfrac{3}{2}a)/(r+1) \tag{7d}$$

Here $a = +1$ for ferromagnetic pair interactions ($J_2 > 0$) and $a = -1$ for antiferromagnetic pair interactions ($J_2 < 0$). For $a = +1$, a little calculation (i.e., find the $\min\{h_i^*\}$) shows that one has to distinguish three cases:

Case F1: $r > 3/2$. The ground states ($T = 0$) are (i) the $(+++)$ *state* (all spins up) for $H^* > (6r - 6)/(r+1)$; (ii) the three ordered

$(+\,+\,-)$ *states* (spins on one sublattice down, spins on the other two up) when $(6r-6)/(r+1) > H^* > 3/(r+1)$; and (iii) the $(-\,-\,-)$ *state* (all spins down) when $H^* < 3/(r+1)$. Thus the ground state undergoes two transitions, one at $H^* = (6r-6)/(r+1)$ and the $(+\,+\,-) \to (-\,-\,-)$ transition at $H^* = 3/(r+1)$. In the former, precisely at $H^* = (6r-6)/(r+1)$, there is an infinite degeneracy of states, so we shall use the notation $(+\,+\,+) \overset{\text{I.D.}}{\to} (+\,+\,-)$ for this transition. This infinite degeneracy has some important implications and it will be shown that these states are in one-to-one correspondence with those of the hard-hexagon model.

Case F2: $r < 3/2$. The ground state undergoes only the $(+\,+\,+) \to (-\,-\,-)$ transition at $H^* = 2r/(r+1)$.

Case F3: $r = 3/2$. Here again we have only one transition at $H^* = 6/5$. When $H^* > 6/5$ we have only the $(+\,+\,+)$ ground state, whereas when $H^* < 6/5$ we have only the $(-\,-\,-)$ ground state. Precisely at $H^* = 6/5$, however, there is an infinite degeneracy of states, and to make this explicit we shall use the notation $(+\,+\,+) \overset{\text{I.D.}}{\to} (-\,-\,-)$ for this transition. The states are not in one-to-one correspondence with the configurations of the hard-hexagon model, but the infinite degeneracy distinguishes the present transition from the $(+\,+\,+) \to (-\,-\,-)$ transition, and has again, as we shall see, some interesting implications.

Using a similar notation we find for antiferromagnetic pair interactions ($a = -1$), the following cases:

Case A1: $r > 1/2$. We have two ground state transitions; the $(+\,+\,+) \overset{\text{I.D.}}{\to} (+\,+\,-)$ at $H^* = 6$ and the $(+\,+\,-) \to (-\,-\,-)$ transition at $H^* = -3/(r+1)$.

Case A2: $r < 1/2$. There are now three transitions. The $(+\,+\,+) \overset{\text{I.D.}}{\to} (+\,+\,-)$ transition at $H^* = 6$; the $(+\,+\,-) \overset{\text{I.D.}}{\to} (-\,-\,+)$ transition at $H^* = -6r/(r+1)$; and the $(-\,-\,+) \overset{\text{I.D.}}{\to} (-\,-\,-)$ transition at $H^* = (6r-6)/(r+1)$.

Case A3: $r = 1/2$. We have again $(+\,+\,+) \overset{\text{I.D.}}{\to} (+\,+\,-)$ transition at $H^* = 6$ and the $(+\,+\,-) \overset{\text{I.D.}}{\to} (-\,-\,-)$ transition at a field $H^* = -2$.

These ground state properties are helpful in understanding the topology of the phase boundaries (since they determine some of their "end points"). Some of the above transitions are expected to extend to finite temperatures (in finite temperatures we drop the notation I.D. and replace the term "state" by the term "phase"). However, the mean-field approximation[5] predicts that in case $F3$ ($r = 3/2$) and also in case $F2$ (for some r) both the $(+\,+\,+) \to (+\,+\,-)$ and the $(+\,+\,-) \to (-\,-\,-)$ transitions occur

at finite temperatures, but our results (Section 4) do not confirm this. Other questions concern the order of these transitions and the slopes of the phase boundaries at their "end points." Some of these questions can be definitely answered. In particular, the $(+++)\to(++-)$ transitions in cases $F1$, $A1$, $A2$, $A3$ and the $(--+)\to(---)$ transition in case $A2$ are of second order and the slope of their phase boundaries at the corresponding critical fields is determined by the critical activity of the hard-hexagon model. To prove this statement let us define

$$T^* = K_B T/(|J_2| + |J_3|) \tag{8a}$$

$$\mathcal{H}^* = \mathcal{H}/(|J_2| + |J_3|) \tag{8b}$$

and transform to lattice gas variables ($\epsilon_i = 0, 1$) by

$$\sigma_i = s(1 - 2\epsilon_i) \qquad (s = \pm 1) \tag{9}$$

Then from (1) and (9) we find

$$\mathcal{H}^* = \sum_{(i,j,k)} \frac{2}{a(r+1)} \left[(2ras - 1)(\epsilon_i\epsilon_j + \epsilon_i\epsilon_k + \epsilon_j\epsilon_k) - 4ras\epsilon_i\epsilon_j\epsilon_k\right]$$
$$- 2\sum_i \left[\frac{6(ras-1)}{a(r+1)} - sH^*\right]\epsilon_i - N\left(sH^* + \frac{3a - 2rs}{r+1}\right) \tag{10}$$

where the first summation is over all $2N$ triangles; the second summation is over all N sites; and as before $a = +1$ for ferromagnetic pair interactions and $a = -1$ for antiferromagnetic. In order to obtain the hard-hexagon lattice gas one must introduce infinite nearest-neighbor repulsions. From (2) and (10) we find that this can be achieved by taking the zero-temperature limit as follows:

$$\frac{sH^*}{T^*} \to \infty \tag{11a}$$

$$\frac{(rsa - 1)}{a(r+1)T^*} \to \infty \tag{11b}$$

$$\frac{(2ras - 1)}{a(r+1)T^*} \to \infty \tag{11c}$$

$$\frac{(2ras - 3)}{a(r+1)T^*} \to \infty \tag{11d}$$

and keeping

$$z = \exp\left\{2\left[\frac{6(ras-1)}{a(r+1)T^*} - \frac{sH^*}{T^*}\right]\right\} \tag{12}$$

fixed. One can verify that the above are satisfied precisely under the conditions that the $(+++) \overset{\text{I.D.}}{\to} (++-)$ $(s = +1)$ and the $(--+)$

$\xrightarrow{\text{I.D.}}(---)$ $(s=-1)$ transitions occur; and that proves the statement that the corresponding infinite degenerate states are in one-to-one correspondence with the configurations of the hard-hexagon model. The critical fields for these transitions ($a=s=1$, $s=-a=1$ and $s=a=-1$, respectively) can be written

$$H_c^* = \frac{6(ras-1)}{as(r+1)} \tag{13}$$

Now, since, as $T^* \to 0$ and $H^* \to H_c^* - (\frac{1}{2}s\ln z)T^*$, the partition function (2) transforms to the partition function of the hard-hexagon model with activity z, it follows that the slope of the phase boundaries $H^*(T^*)$ at $T=0$

$$\lambda = \left.\frac{dH^*(T^*)}{dT^*}\right|_{T^*=0} \tag{14}$$

is related to the critical activity of the hard-hexagon model[6] by

$$\lambda = -\frac{s}{2}\ln z_c = -\frac{s}{2}\ln\left[\frac{1}{2}(11+5\sqrt{5})\right] \tag{15}$$

Furthermore, the critical magnetization is related to the critical density of hard hexagons by[6]

$$|M_c| = 1 - 2\rho_c = 0.447\ldots \tag{16}$$

Precisely at $r=\frac{3}{2}$ $(r=\frac{1}{2})$ in case $F3$ $(A3)$, the limits (11d) [(11c)] cannot be satisfied and the one-to-one correspondence with the hard-hexagons configurations does not hold. However, the implications of the infinite degeneracy of states will be discussed in Section 4, where we present the results of the variational method.

3. VARIATIONAL APPROXIMATIONS

The matrix equations for "antiferromagnetic" triangular models are given in Eqs. (6) and (7) of I. Using a representation in which the corner transfer matrices $B(a)$ and $\tilde{A}(a)$ are diagonal we can write these equations as

$$\sum_b F(a,b)\tilde{A}(b)F(b,a) = \xi_1\tilde{A}^2(a) \tag{17a}$$

$$\sum_b \tilde{G}^T(b,a)\tilde{G}(b,a) = \xi_2 B^4(a) \tag{17b}$$

$$\sum_b \tilde{G}(a,b)B^2(b)\tilde{G}^T(a,b) = \xi_3\tilde{A}^3(a) \tag{17c}$$

$$\sum_c w(a,b,c)F(a,c)\tilde{G}(c,b) = \eta_1^{1/2}\tilde{G}(a,b)B(b) \tag{17d}$$

$$\sum_c w(a,b,c)\tilde{G}(a,c)B(c)\tilde{G}^T(b,c) = \eta_3^{1/2}\tilde{A}(a)F(a,b)\tilde{A}(b) \tag{17e}$$

$$F(a,b) = F^T(b,a) \tag{17f}$$

Here a, b, and c have values ± 1; and $w(a,b,c)$ is the Boltzmann weight of the interacting spins a, b, and c surrounding an elementary triangle. The partition function per site is

$$k = \left\{(\eta_1^2\eta_3)/(\xi_1\xi_2\xi_3)\right\}^{1/3} \tag{18}$$

Furthermore, the magnetizations can be expressed in terms of the corner transfer matrices (they have been obtained from a variational expression for k in I):

$$M = \tfrac{2}{3}m + \tfrac{1}{3}m' \tag{19a}$$

$$m = \frac{\sum_a a \operatorname{Tr}\left[\tilde{A}^3(a)\right]}{\sum_a \operatorname{Tr}\left[\tilde{A}^3(a)\right]} \tag{19b}$$

$$m' = \frac{\sum_a a \operatorname{Tr}\left[B^6(a)\right]}{\sum_a \operatorname{Tr}\left[B^6(a)\right]} \tag{19c}$$

Here m' is the magnetization for the sublattice distinguished from the other two.

In cases where the lattice symmetry is not broken the infinite-dimensional solution of Eqs. (17) is expected to have the properties

$$\tilde{A}(a) = B^2(a) = A^2(a) \tag{20a}$$

$$\tilde{G}(a,b) = A(a)F(a,b) \tag{20b}$$

$$\xi_1 = \xi_2 = \xi_3 = \xi, \qquad \eta_1 = \eta_3 = \eta \tag{20c}$$

and our equations reduce to those given by Baxter and Tsang[11]:

$$\sum_b F(a,b)A^2(b)F(b,a) = \xi A^4(a) \tag{21a}$$

$$\sum_c w(a,b,c)F(a,c)A(c)F(c,b) = \eta^{1/2}A(a)F(a,b)A(b) \tag{21b}$$

$$F(a,b) = F^T(b,a) \tag{21c}$$

$$k = \eta/\xi \tag{21d}$$

$$M = m = m' = \frac{\sum_a a \operatorname{Tr}\left[A^6(a)\right]}{\sum_a \operatorname{Tr}\left[A^6(a)\right]} \tag{21e}$$

In the following section we utilize these equations to study the phase

diagrams for the model (1) with ferromagnetic pair interactions ($J_2 > 0$) for several values of $r(= |J_3|/|J_2|)$. The $n_1 \times n_2$ approximation truncates $\tilde{A}(+)$, $B(+)$, $F(+,+)$, and $\tilde{G}(+,+)$ to be $n_1 \times n_1$; $F(+,-)$ and $\tilde{G}(+,-)$ $[F(-,+)$ and $\tilde{G}(-,+)]$ to be $n_1 \times n_2(n_2 \times n_1)$; and $\tilde{A}(-)$ and $B(-)$ to be $n_2 \times n_2$ matrices. The resulting nonlinear algebraic equations are solved by the Newton–Raphson method. Initial guesses are obtained using the "eigenvalue iterative procedure" of Baxter[7] as generalized in I.

4. PHASE DIAGRAMS

We consider first the 1×1 approximation (all matrices 1×1) and derive phase diagrams for several values of r. These phase diagrams (Figs. 1a–1e) are obtained as follows. In the general case, $r > 3/2$, we find three physically interesting solutions [the solution of Eqs. (17) is not unique and one has to select the solution that maximizes k]. Using a notation reflecting the low-temperature properties of these solutions we shall refer to them as the $(+++)$, $(---)$, and $(++-)$ solutions. The $(+++)$ and the $(---)$ solutions satisfy the symmetry properties (20); the $(++-)$ solution does not. Let the partition function per site k, corresponding to these solutions, be denoted by $k(+++)$, $k(---)$, and $k(++-)$, respectively. The phase boundaries are determined by comparing these partition functions in the (H^*, T^*) plane. The critical lines (P_1P_3), (P_2P_3), and (P_3P_4) are determined by the conditions $k(+++) = k(++-)$, $k(++-) = k(---)$, and $k(+++) = k(---)$, respectively. For $r > 3/2$ the three solutions satisfy at P_3: $k(+++) = k(++-) = k(---)$. The solution that maximizes k in each region is indicated in Fig. 1b.

In Figs. 1a–1e the mean-field approximation[5] is also shown by dotted lines. The 1×1 approximation yields the exact "end points" given by the ground state considerations:

$$H_c^* = H_{P_1}^* = (6r - 6)/(r + 1) \qquad \text{for } r > 3/2 \tag{22a}$$

$$H_{P_2}^* = 3/(r + 1) \qquad \text{for } r > 3/2 \tag{22b}$$

$$H_{P_3}^* = 2r/(r + 1) \qquad \text{for } r \leqslant 3/2 \tag{22c}$$

From Figs. 1a–1e, one can see that the quantitative predictions of the mean-field approximation are very poor. Qualitatively the mean field has some drawbacks not shared with the 1×1 approximation. It predicts a positive value for the slope λ and thus two transitions for certain values of H^* (above $H_{P_1}^*$), one transition from the $(+++)$ to the $(++-)$ phase and another, in some higher temperature, from the $(++-)$ to the $(+++)$ phase. It also predicts[5] that the $(+++) \rightarrow (++-)$ and the $(++-)$ $\rightarrow (---)$ transitions occur even for some $r \leqslant 3/2$. The 1×1 approximation rules out these possibilities as it can be seen from Figs. 1a–1e.

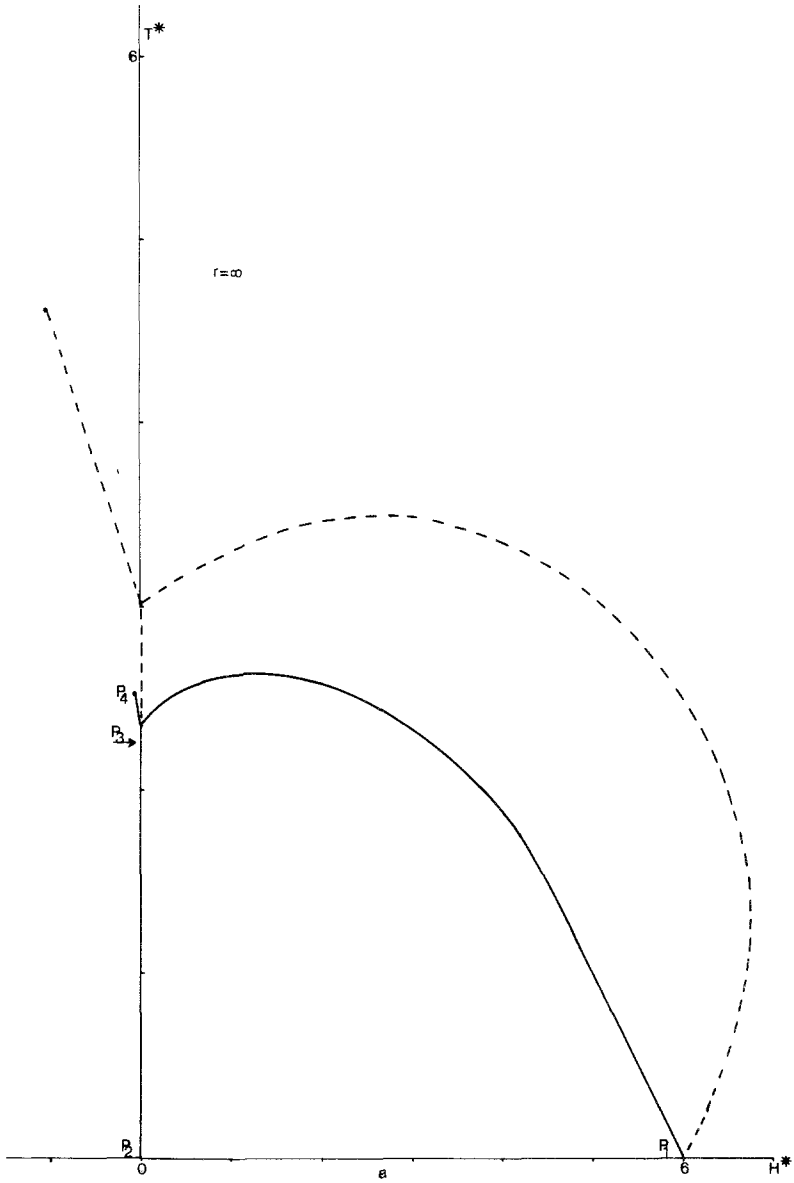

Fig. 1. Phase diagrams of the triangular Ising model (1) with ferromagnetic pair interactions for varying strengths of the pair and triplet interactions. Solid lines (this work, 1×1 approximation), dashed lines (Ref. 5, mean-field approximation). Arrows indicate exact (zero-field) results.

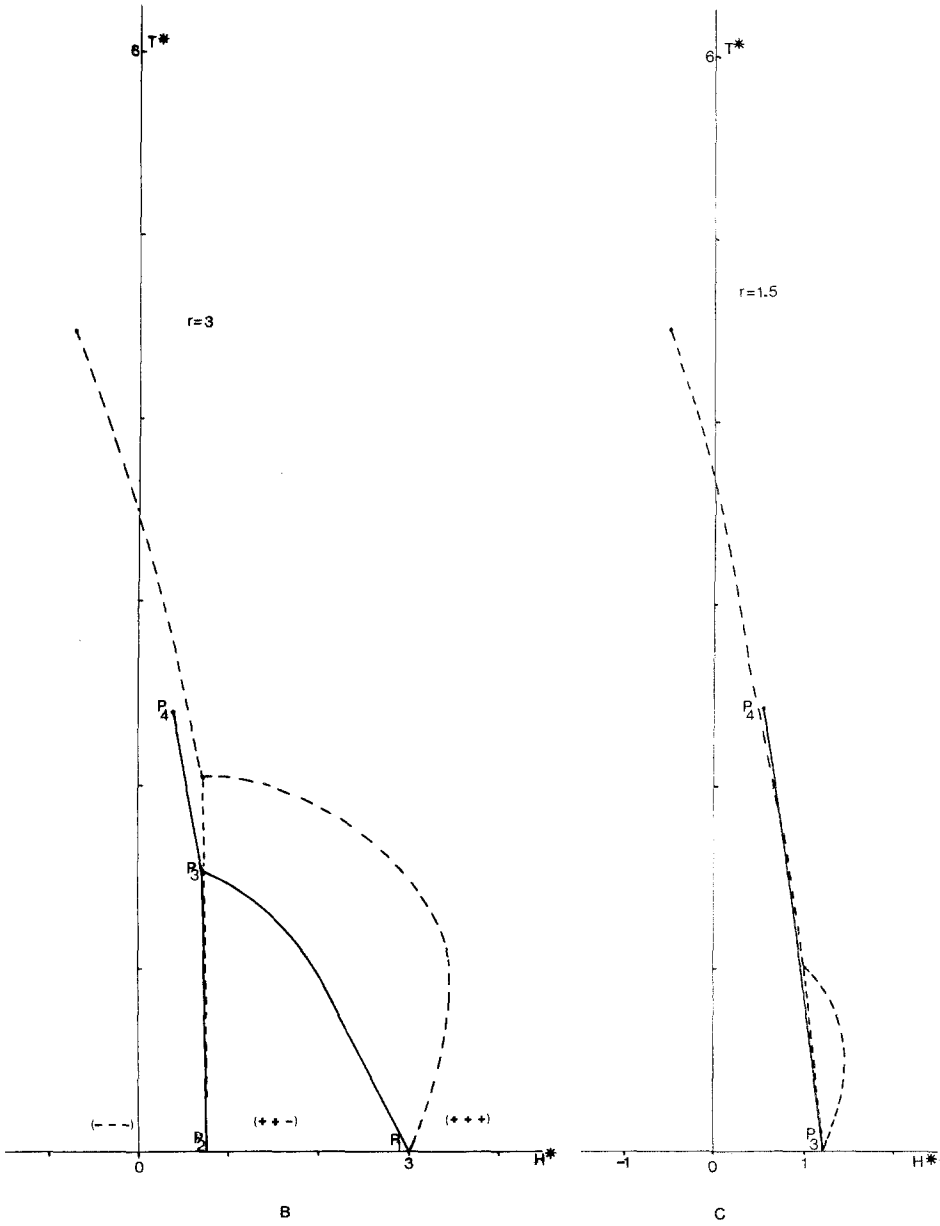

Fig. 1. (*continued*)

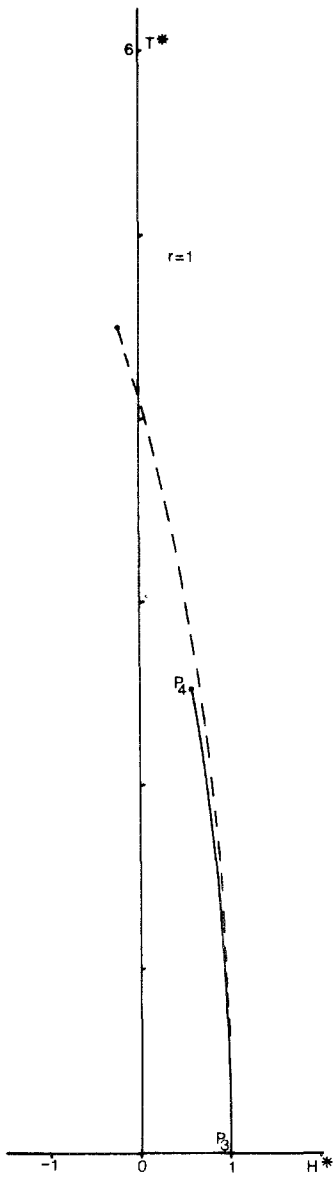

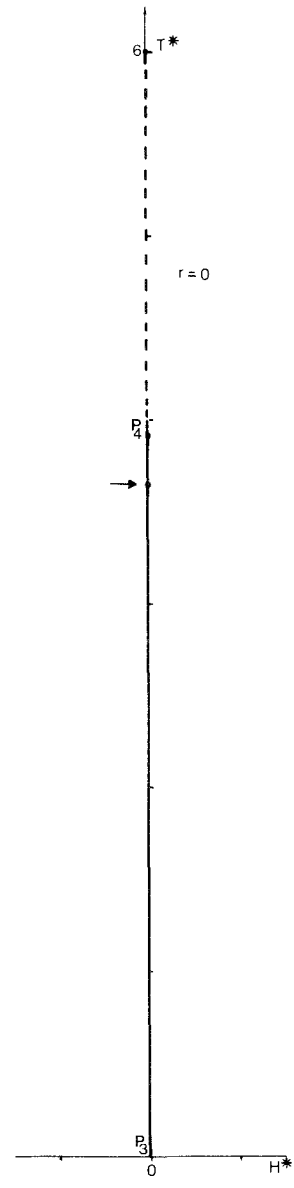

Fig. 1. (*continued*)

The slope of the line (P_1P_3) at the critical field, $H^*_{P_1}$, is independent of the value of r (as it should be) and is a reasonable approximation ($\lambda_{1\times1} = -1.02\ldots$) to the exact result ($\lambda = -1.203\ldots$).

Regarding the nature of phase transitions the 1×1 approximation gives, in general, first-order transitions with jumps in magnetization; P_4 being a "classical" critical point within the approximation. The jumps are small only for the critical line (P_1P_3). From the magnitude of the jumps one could conclude that the $(+++)\to(---)$ and the $(++-)\to(---)$ transitions are of first order, whereas the $(++-)\to(+++)$ transition is of second order. As $T^*\to0$, the $(---)\to(++-)$ transition takes place between magnetizations -1 and $+1/3$; the slope of the phase boundary at P_2 is independent of r and it is zero ($dH^*/dT^*|_{T^*=0} = 0$). For $r < 3/2$ the "ferromagnetic" $(+++)\to(---)$ transition takes place, as $T^*\to0$, between magnetizations $+1$ and -1; again the slope is independent of r and it is zero. However, precisely at $r = 3/2$ the ferromagnetic $(+++)\to(---)$ transition takes place, as $T^*\to0$, between magnetizations $0.6447\ldots$ and -1 and the slope of the phase boundary is nonzero: $dH^*/dT^*|_{T^*=0} = -0.2$. We suppose that this rather surprising result is not an artifact of the 1×1 approximation. It seems reasonable to speculate that this different behavior is due to the infinite degeneracy of ground states pointed out in Section 2 (case $F3$). For $r > 3/2$ the ferromagnetic $(+++)\to(---)$ transition at P_3 takes place between a positive and a negative magnetization, both varying with r.

It should be pointed out that the "length" of the line (P_3P_4) for $r = \infty$ $(J_2 = 0)$ is of the order of the error of the 1×1 approximation. It is therefore possible that P_3 and P_4 coincide in the exact solution. Indeed, this seems to be the case since in the 2×2 approximation (P_3P_4) becomes "shorter" and is again of the order of the error of the 2×2 approximation. However, for $3/2 < r < \infty$ the line (P_3P_4) does not seem to be merely an artifact of the approximation (Fig. 1b); this can also be seen from Table I, where we give the points P_3 and P_4 for several values of r. It is therefore possible that in the exact solution $H^*_{P_4} \geqslant 0$ for any r; note that mean field yields $H^*_{P_4} \leqslant 0$ for any r.

We restrict now the treatment to pure triplet interactions $(J_2 = 0)$ and present two higher approximations to the critical line (P_1P_3). These are the 2×2 and 3×2 approximations shown in Fig. 2 together with the 1×1 approximation. The numerical results are given in Table II. They converge to the exact values, as can be seen by comparing with the exactly solvable zero-field case and also with the hard-hexagon result (15). The 2×2 approximation yields $\lambda_{2\times2} = -1.16\ldots$ and the 3×2: $\lambda_{3\times2} = -1.206\ldots$, in good agreement with the exact result ($\lambda = -1.203\ldots$). The jumps in magnetization are, in general, small in magnitude and tend to zero as the size of the matrices tends to infinity, so the $\infty\times\infty$ solution would yield, as

Table I. Results of the 1×1 Approximation for the "End Points" of the Phase Diagrams P_3 and P_4 for Several Values of r

$r = \lvert J_3\rvert/\lvert J_2\rvert$	$T^*_{P_3}$	$H^*_{P_3}$	$T^*_{P_4}$	$H^*_{P_4}$
∞	$2.347\ldots$ [a]	0	$2.524\ldots$	$-0.072\ldots$
20	$2.229\ldots$	$0.135\ldots$	$2.492\ldots$	$0.027\ldots$
3	$1.528\ldots$	$0.712\ldots$	$2.408\ldots$	$0.38\ldots$
2	$0.92\ldots$	$0.966\ldots$	$2.408\ldots$	$0.481\ldots$
1.5	0 [b]	1.2 [b]	$2.435\ldots$	$0.532\ldots$
1	0 [b]	1 [b]	$2.524\ldots$	$0.555\ldots$
0.5	0 [b]	2/3 [b]	$2.83\ldots$	$0.454\ldots$
0.2	0 [b]	1/3 [b]	$3.312\ldots$	$0.245\ldots$
0	0 [b]	0 [b]	$3.915\ldots$ [c]	0

[a] Exact result: $2/\ln(1/\sqrt{2}) = 2.269\ldots$.
[b] Exact results given in Eq. (22c).
[c] Exact result: $4/\ln 3 = 3.640\ldots$.

expected, second-order transitions for (P_1P_3). The jump is maximal at $H^* = 0$, but, even in this apparently least accurate case for the magnetization, the trend of the results is correct [the 1×1 results for $H^* = 0$ are $M(++-) = 0.281$ and $M(+++) = 0$]. The jump is zero at $H^* \simeq 1.5$, where it also changes sign. Comparing the values of the magnetizations in Table II one can see that $M(++-)$ is more accurate than $M(+++)$ (away from zero field). The limiting values of $M(++-)$ as we approach the critical field ($H^* = 6$) are 0.44 and 0.43 for the 2×2 and 3×2 approximations, respectively, in very good agreement with the exact result (16). Apparently, away from zero field, the 2×2 approximation for $M(++-)$ is accurate to the second decimal place.

For pure triplet interactions, Baxter, Sykes, and Watts[4] have conjectured an expression for the magnetization along (P_2P_3), with a critical exponent $\beta_M = 1/12$. The magnetizations of the $(---)$ and $(++-)$ phases along this line are related by $M(---) = -3M(++-)$ as we can show from Eqs. (17). Indeed, at $H^* = 0$ we have $w(a,b,c) = w(-a,-b,c)$ and if Eqs. (17) have a solution $\tilde{A}, B, F, \tilde{G}$ they also permit a solution $\tilde{A}^*, B^*, F^*, \tilde{G}^*$, where

$$A^*(a) = \tilde{A}(-a), \qquad B^*(a) = B(a) \tag{23a}$$

$$F^*(a,b) = F(-a,-b), \qquad \tilde{G}^*(a,b) = \tilde{G}(-a,b) \tag{23b}$$

$$k^* = k \tag{23c}$$

Considering $\tilde{A}, B, F, \tilde{G}$ to describe the $(---)$ phase, the $\tilde{A}^*, B^*, F^*, \tilde{G}^*$ solution describes the $(++-)$ phase. It is reasonable to assume that the

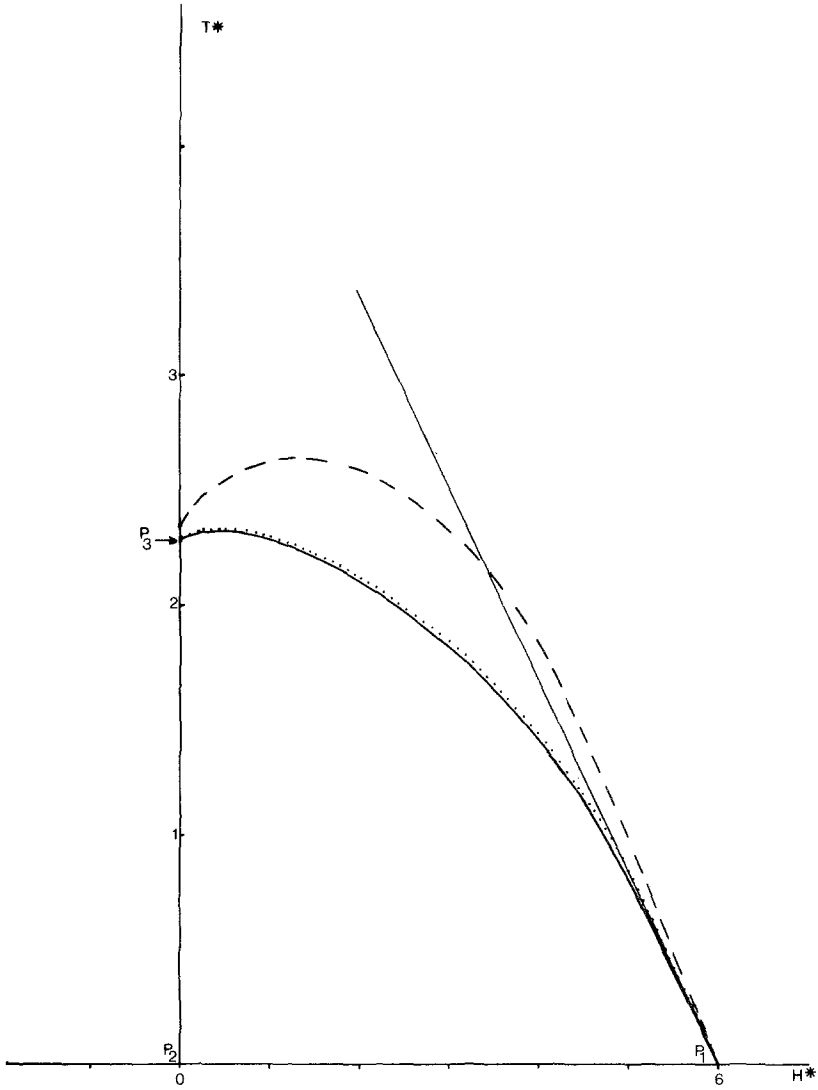

Fig. 2. Phase diagrams for the case of pure triplet interactions ($J_2 = 0$). Solid line (3×2 approximation), dotted line (2×2 approximation), dashed line (1×1 approximation). The straight line shows that exact slope at $H^* = 6$. Arrow indicates the exact Baxter–Wu critical temperature.

Table II. Variational Approximations for the Critical Line (P_1P_3) in the Case of Pure Triplet Interactions

	2×2 Approximation			3×2 Approximation		
H^*	T^a	$M(++-)$	$M(+++)$	T^a	$M(++-)$	$M(+++)$
0	2.284†	0.251	0	2.278†	0.260	0.107
0.5	2.336	0.297	0.268	2.321	0.302	0.278
1	2.298	0.319	0.307	2.280	0.321	0.312
1.5	2.223	0.335	0.334	2.203	0.336	0.335
2	2.120	0.350	0.357	2.099	0.350	0.356
2.5	1.993	0.365	0.378	1.970	0.363	0.374
3	1.839	0.379	0.399	1.815	0.375	0.391
3.5	1.656	0.395	0.420	1.631	0.388	0.409
4	1.438	0.410	0.442	1.412	0.402	0.427
4.5	1.171	0.426	0.463	1.145	0.415	0.443
5	0.836	0.444	0.481	0.812	0.425	0.456
5.5	0.428	0.444	0.487	0.414	0.428	0.460

[a] Exact result: $2/\ln(1+\sqrt{2}) = 2.2691\ldots$.

$\infty \times \infty$ solution that maximizes k for the $(---)$ phase will satisfy the symmetry properties (20) so that $m = m'$ and from (23) and (19) we find $M(---) = -3M(++-)$.

5. COMPUTATIONAL REMARKS

In general each of the solutions [$(+++)$, $(---)$, and $(++-)$ solutions], used to obtain the phase boundaries in the previous section exists in the region where it maximizes k but also a little outside this region. A similar situation was found by Baxter, Enting, and Tsang[12] in their study of the hard-square lattice gas. It is expected[12] that this interpenetration of the solutions will disappear as the size of the matrices increases. It may be speculated that the line (P_3P_4), in the case of pure triplet interactions, is a consequence of this interpenetration of the "finite" solutions and will shrink to a single point (P_3) as the size of the matrices increases.

The $\infty \times \infty$ solution of the matrix equations defining the variational approximations [in our case Eqs. (17)], that maximizes k, is expected, in some cases, to satisfy certain symmetry properties [such as (20)]. However, it should be pointed out that this need not be true in all finite-order approximations not even for the "square" $(n_1 = n_2)$ approximations. A striking example is the 2×2 approximation for $H^* = J_2 = 0$. In this case we found two solutions for the $(---)$ phase, one symmetric [i.e., satisfying (20)] and an asymmetric [not satisfying (20)]; the asymmetric solution

maximizes k. The difference between these solutions is small and presumably will diminish as one goes to higher approximations. From the symmetric $(---)$ solution we then obtained using (23) a "symmetric" $(++-)$ solution (with $m = -m'$ at $H^* = 0$), which then becomes asymmetric as H^* increases. It is therefore possible to obtain a 2×2 approximation to the critical line (P_3P_1) starting from the "symmetric" $(++-)$ solution; the results are then slightly different from those in Table II. For instance, this yields $T^*(H^* = 0) = 2.2828\ldots$, whereas the asymmetric yields $T^*(H^* = 0) = 2.2840\ldots$; the asymmetric solution gives slightly smaller jumps in magnetization. In the 1×1 approximation the $(---)$ solution that maximizes k satisfies also the symmetry properties (20).

6. CONCLUDING REMARKS

We have explored the implications of the known hard-hexagon lattice gas results for the triangular Ising model with both pair and triplet interactions. The model has been studied by the variational method when the pair interactions are ferromagnetic and the nature of phase diagrams has been clarified. The numerical results of the approximations are in good agreement with the known exact results and higher approximations converge to the exact values as indicated by the 2×2 and 3×2 approximations for the case of pure triplet interactions. The lowest-order 1×1 approximation yields successful qualitative predictions. It predicted that the slope of the $(+++) \to (++-)$ phase boundary at the critical field and the critical magnetization are independent of r (the ratio of the interaction strengths). It points out that the $T^* = 0$ slope of the phase boundaries for the $(+++) \to (---)$ $(r < 3/2)$ and the $(++-) \to (---)$ $(r > 3/2)$ transitions is also independent of r and it is zero. We conjecture this to be an exact result. Finally, for the special ratio $r = 3/2$ it predicts that the $(+++) \to (---)$ transition takes place, as $T^* \to 0$, between magnetizations $0.6447\ldots$ and -1 and the slope of the phase boundary has a nonzero value, i.e., -0.2. It is reasonable to assume that the numerical values 0.64 and -0.2 are only approximate; however, we expect the qualitative prediction, that the $(+++) \to (---)$ transition at $r = 3/2$ is different (at low temperatures) from the $(+++) \to (---)$ transition for $r < 3/2$, to be correct.

ACKNOWLEDGMENT

I wish to thank Professor P. C. Hemmer for helpful discussions and NTNF for a fellowship.

REFERENCES

1. D. Merlini, A. Hintermann, and Ch. Gruber, *Lett. Nuov. Cim.* **7**: 815 (1973).
2. D. W. Wood and H. P. Griffiths, *J. Phys. C* **7**: 1417 (1974).
3. R. J. Baxter and F. Y. Wu, *Phys. Rev. Lett.* **31**: 1294 (1973); *Aust. J. Phys.* **27**: 357 (1974).
4. R. J. Baxter, M. F. Sykes and M. G. Watts, *J. Phys. A* **8**: 245 (1975).
5. S. Frøyen, Aa. S. Sudbø, and P. C. Hemmer, *Physica* **85A**: 399 (1976).
6. R. J. Baxter, *J. Phys. A* **13**: L61 (1980).
7. R. J. Baxter, *J. Stat. Phys.* **19**: 461 (1978).
8. R. J. Baxter, *J. Math. Phys.* **9**: 650 (1968).
9. S. B. Kelland, *Can. J. Phys.* **54**: 1621 (1976).
10. R. J. Baxter and I. G. Enting, *J. Stat. Phys.* **21**: 103 (1979).
11. R. J. Baxter and S. K. Tsang, *J. Phys. A* **13**: 1023 (1980).
12. R. J. Baxter, I. G. Enting and S. K. Tsang, *J. Stat. Phys.* **22**: 465 (1980).
13. A. Malakis, *Ark. Fys. Semin. Trondheim* **No. 13** (1980).